

# We are IntechOpen, the world's leading publisher of Open Access books Built by scientists, for scientists

4,800

Open access books available

122,000

International authors and editors

135M

Downloads

Our authors are among the

154

Countries delivered to

TOP 1%

most cited scientists

12.2%

Contributors from top 500 universities



WEB OF SCIENCE™

Selection of our books indexed in the Book Citation Index  
in Web of Science™ Core Collection (BKCI)

Interested in publishing with us?  
Contact [book.department@intechopen.com](mailto:book.department@intechopen.com)

Numbers displayed above are based on latest data collected.

For more information visit [www.intechopen.com](http://www.intechopen.com)



# Radiation and Energy Flux of Electromagnetic Fields by a Segment of Relativistic Electron Beam Moving Uniformly in Vacuum

*Sergey Prijmenko and Konstantin Lukin*

## Abstract

A finite-length segment of filamentous relativistic electron beam (REB), moving uniformly in vacuum, radiates hybrid electromagnetic waves, compound of potential and vortex electric fields, as well as a vortex magnetic field. The strengths of electric and magnetic fields radiated by the segment edges have the opposite signs. The electromagnetic fields in the wave zone are considered as superposition of the electromagnetic waves radiated by the beginning and the end of the REB segment, which, in particular, leads to formation of the field's interference components. In both the near and the intermediate zones, there is a flow of electrical energy due to the electric potential field and the field of displacement current.

**Keywords:** relativistic electron beam or REB segment, potential field, vortex field, radiation of EM waves, near field zone, intermediate zone and far field (wave) zone, EM energy flux

## 1. Introduction

The physics of charged particle beam is an area where relativistic effects manifest themselves substantially. Here, one has to deal with a moving object, so both a fixed (laboratory) coordinate system and a moving coordinate system are to be used. A charged particle moves relative to the laboratory coordinate system, while in the moving coordinate system, it is at rest. Hence, in a laboratory coordinate system, the problem is to be considered as an electrodynamic one, and in a moving coordinate system, the problem belongs to the area of electrostatics. Thus, electrostatic phenomena in a charged particle set at rest are transformed into electrodynamic ones when it moves. Electromagnetic fields in these two inertial reference systems are tied via the Lorentz transform ([1], p. 79).

In the wave zone, the dynamic component of the electric field strength and the axially symmetric magnetic field form both a constant flux into a given solid angle, i.e., electromagnetic radiation, and a flux per time unit directed along the normal to the conical surface of the solid angle. The potential component of the electric field, directed along the radius, and the axially symmetric magnetic field form a flux oriented along the polar direction, i.e., along the normal to the above conical surface. The fluxes crossing the conical surface do not depend on the distance between the source point and the observation point. In the wave zone, the

radiations from the beginning and end of the REB segment are added up, while the fluxes through the above conical surface caused by dynamic and potential components of electric field, are subtracted.

To date, the issue of influence of the finite length of a charged particle beam, moving uniformly in vacuum on the radiation of electromagnetic fields remains poorly studied, with an exception of publication [2], where its experimental part deserves special attention.

This chapter presents the results of our theoretical analysis of the electromagnetic field radiated by a finite-length segment of filamentous relativistic electron beam (REB). The REB segment moves uniformly in vacuum along its own axis which we will address as the *longitudinal direction*. The stepped varying of the charge density at the edges of the REB segment creates point-like sources of the potential electric field; the strength of which is inversely proportional to the distance between the source point and the observation point. In addition, the time variation of the REB current density forms at the REB edges the point-like sources of both potential and vortex electric fields, as well as the vortex magnetic field, with their strengths being also inversely proportional to the distance between the source point and the observation point [3].

The filamentary REB edges are considered as relativistic point-like radiators of the electromagnetic energy propagating to the wave zone. The presence of a potential electric field in the wave zone is due to the fact that the electric scalar potential in the wave zone is proportional to the electric *monopole* moment ([4], p. 51), which equals to the total charge in the selected volume ([5], p. 280). As follows from the Jefimenko's generalization of the Coulomb law ([3], p. 246), the potential electric field strength in the wave zone is proportional to the time derivative of the electric monopole moment.

In the intermediate zone, there is a flow of electrical field energy, due to the electric potential field and the field of the displacement current. The electrical energy flux in the intermediate zone is due to the electric potential field and field of the displacement current. The REB part with a constant charge density between its edges forms a quasi-static electromagnetic field in the near zone.

Note that a similar problem has been considered in [6], but it was devoted to similarity of the solutions obtained with the help of two different methods: retarded field integral and transformation equations of the special theory of relativity. Unlike our work, it does not contain expressions for scalar and vector potentials, as well as the electromagnetic energy flux.

## 2. Formulation of the problem

Consider a filamentary REB segment of length  $L$  and electric charge density  $Q$  moving uniformly along its axis direction with velocity  $v_e$ . Charge density of the REB segment may be written as follows:

$$\rho(\mathbf{t}, \mathbf{r}(x, y, z))_L = \frac{Q}{L} \delta(x) \cdot \delta(y) \cdot [h(z - v_e t) - h(z - (v_e t + L))] \quad (1)$$

where  $h(x)$  is Heaviside step function;  $\delta(x)$  and  $\delta(y)$  are Dirac delta functions of coordinates. The electric scalar potential  $\psi(\mathbf{t}, \mathbf{r})$  and vector potential  $\vec{A}(\mathbf{t}, \mathbf{r})$ , taking into account Eq. (1), satisfy the wave equations [3, 7]:

$$\left[ \text{divgrad} - \frac{1}{c^2} \frac{\partial^2}{\partial t^2} \right] \psi(\mathbf{t}, \mathbf{r}) = -\frac{\rho(\mathbf{t}, \mathbf{r})}{\epsilon_0}, \quad (2)$$

$$\left[ \text{grad div} - \text{rot rot} - \frac{1}{c^2} \frac{\partial^2}{\partial t^2} \right] \vec{A}(t, r) = -\mu_0 \rho(t, r) v_e \vec{k}_0, \quad (3)$$

where  $\epsilon_0$  and  $\mu_0$  are the dielectric and magnetic permeability of vacuum, respectively; and  $\vec{k}_0$  is the unit vector along the REB axis, the Oz axis.

### 3. Potentials

A potential part of the vector potential  $\vec{A}^P(t, r)$  is related to the scalar potential by the Lorentz calibration [3, 7]:

$$\text{div} \vec{A}^P(t, r) = -\frac{1}{c^2} \frac{\partial}{\partial t} \psi(t, r), \quad (4)$$

Using the Green's function for the wave equation ([3], p. 243), we obtain:

$$\begin{aligned} \psi(t', x' = 0, y' = 0, v_e t' < z' < v_e t' + L; t, r(x, y, z)) &= \\ &= -\frac{Q}{L4\pi\epsilon_0} \int_{v_e t'}^{v_e t' + L} \frac{dz'}{\sqrt{x^2 + y^2 + (z - z')^2}} \Bigg|_{t' = t - \frac{|\vec{r} - \vec{r}'|}{c}}, \end{aligned} \quad (5)$$

$$\begin{aligned} \vec{A}(t', x' = 0, y' = 0, v_e t' < z' < v_e t' + L; t, r(x, y, z)) &= \\ &= -\frac{Q\mu_0}{L4\pi} \int_{v_e t'}^{v_e t' + L} \frac{dz'}{\sqrt{x^2 + y^2 + (z - z')^2}} \Bigg|_{t' = t - \frac{|\vec{r} - \vec{r}'|}{c}}, \end{aligned} \quad (6)$$

where the hatched coordinates refer to the source point at the time instant  $t'$  of the field radiation, and the non-hatched coordinates refer to the observation point at the time instant  $t$ .

The formula for the scalar potential can be obtained in the closed form using the table integral ([8], p. 34):

$$\begin{aligned} \psi(t', x' = 0, y' = 0, v_e t' < z' < v_e t' + L; t, r(x, y, z)) &= \\ &= \frac{Q}{L4\pi\epsilon_0} \ln \left| (z - (v_e t' + L)) + \sqrt{x^2 + y^2 + (z - (v_e t' + L))^2} \right| \Bigg|_{t' = t - \frac{|\vec{r} - \vec{r}'(t', z' = v_e t' + L)|}{c}} \\ &\quad - \frac{Q}{L4\pi\epsilon_0} \ln \left| (z - v_e t') + \sqrt{x^2 + y^2 + (z - v_e t')^2} \right| \Bigg|_{t' = t - \frac{|\vec{r} - \vec{r}'(t', z' = v_e t')|}{c}} \end{aligned} \quad (7)$$

where the expressions in the first and second summands refer to the REB segment end and its beginning, respectively.

### 4. The electromagnetic field strengths

For estimation of the electric and magnetic fields, we use standard formulas ([7], p. 432):

$$\begin{aligned} & \vec{E}(t', x' = 0, y' = 0, v_e t' < z' < v_e t' + L; t, r(x, y, z)) = \\ & = - \frac{\vec{\partial} \vec{A}(t', x' = 0, y' = 0, v_e t' < z' < v_e t' + L; t, r(x, y, z))}{\partial t} \\ & - \text{grad}_r \psi(t', x' = 0, y' = 0, v_e t' < z' < v_e t' + L; t, r(x, y, z)), \end{aligned} \quad (8)$$

$$\begin{aligned} & \vec{H}(t', x' = 0, y' = 0, v_e t' < z' < v_e t' + L; t, r(x, y, z)) = \\ & = \frac{1}{\mu_0} \text{rot}_r \vec{A}(t', x' = 0, y' = 0, v_e t' < z' < v_e t' + L; t, r(x, y, z)), \end{aligned} \quad (9)$$

where it is necessary to perform the differentiation over the coordinates of the observation point, taking into account the retardation effect ([7], p. 432) and ([4], p. 43) as well as the differentiation of integrals by the integration limits and by the parameter ([9], p. 58). Using Eqs. (5), (6), and (8), we get:

$$\begin{aligned} & E_x^p(t', x' = 0, y' = 0, v_e t' < z' < v_e t' + L; t, r(x, y, z)) = \\ & = \frac{Qv_e}{L4\pi\epsilon_0 c} \frac{\cos [\alpha_x(z' = v_e t')]}{\kappa(z' = v_e t')} \left| \vec{r} - \vec{r}'(t', z' = v_e t') \right|_{t'=t - \frac{|\vec{r} - \vec{r}'(t', z' = v_e t')|}{c}} - \\ & - \frac{Qv_e}{L4\pi\epsilon_0 c} \frac{\cos [\alpha_x(z' = v_e t' + L)]}{\kappa(z' = v_e t' + L)} \left| \vec{r} - \vec{r}'(t', z' = v_e t' + L) \right|_{t'=t - \frac{|\vec{r} - \vec{r}'(t', z' = v_e t' + L)|}{c}} + \\ & + \frac{Q}{L4\pi\epsilon_0} \int_{v_e t'}^{v_e t' + L} \frac{\cos [\alpha_x(z')]}{\left| \vec{r} - \vec{r}'(t', z') \right|_{t'=t - \frac{|\vec{r} - \vec{r}'(t', z')|}{c}}^2} dz' \end{aligned} \quad (10)$$

$$\begin{aligned} & E_y^p(t', x' = 0, y' = 0, v_e t' < z' < v_e t' + L; t, r(x, y, z)) = \\ & = \frac{Qv_e}{L4\pi\epsilon_0 c} \frac{\cos [\alpha_y(z' = v_e t')]}{\kappa(z' = v_e t')} \left| \vec{r} - \vec{r}'(t', z' = v_e t') \right|_{t'=t - \frac{|\vec{r} - \vec{r}'(t', z' = v_e t')|}{c}} - \\ & - \frac{Qv_e}{L4\pi\epsilon_0 c} \frac{\cos [\alpha_y(z' = v_e t' + L)]}{\kappa(z' = v_e t' + L)} \left| \vec{r} - \vec{r}'(t', z' = v_e t' + L) \right|_{t'=t - \frac{|\vec{r} - \vec{r}'(t', z' = v_e t' + L)|}{c}} + \\ & + \frac{Q}{L4\pi\epsilon_0} \int_{v_e t'}^{v_e t' + L} \frac{\cos [\alpha_y(z')]}{\left| \vec{r} - \vec{r}'(t', z') \right|_{t'=t - \frac{|\vec{r} - \vec{r}'(t', z')|}{c}}^2} dz' \end{aligned} \quad (11)$$

$$\begin{aligned} & E_z^p(t', x' = 0, y' = 0, v_e t' < z' < v_e t' + L; t, r(x, y, z)) = \\ & = \frac{Qv_e}{L4\pi\epsilon_0 c} \frac{\cos [\alpha_z(z' = v_e t')]}{\kappa(z' = v_e t')} \left| \vec{r} - \vec{r}'(t', z' = v_e t') \right|_{t'=t - \frac{|\vec{r} - \vec{r}'(t', z' = v_e t')|}{c}} - \\ & - \frac{Qv_e}{L4\pi\epsilon_0 c} \frac{\cos [\alpha_z(z' = v_e t' + L)]}{\kappa(z' = v_e t' + L)} \left| \vec{r} - \vec{r}'(t', z' = v_e t' + L) \right|_{t'=t - \frac{|\vec{r} - \vec{r}'(t', z' = v_e t' + L)|}{c}} \end{aligned}$$

$$\begin{aligned}
 & - \frac{Q\mu_0 v_e^2}{L4\pi} \frac{1}{\kappa(z' = v_e t') \left| \vec{r} - \vec{r}'(t', z' = v_e t') \right| \Big|_{t'=t - \frac{|\vec{r} - \vec{r}'(t', z' = v_e t')|}{c}}} + \\
 & + \frac{Q\mu_0 v_e^2}{L4\pi} \frac{1}{\kappa(z' = v_e t' + L) \left| \vec{r} - \vec{r}'(t', z' = v_e t' + L) \right| \Big|_{t'=t - \frac{|\vec{r} - \vec{r}'(t', z' = v_e t' + L)|}{c}}} + \\
 & + \frac{Q}{L4\pi\epsilon_0} \int_{v_e t'}^{v_e t' + L} \frac{\cos [\alpha_z(z')] \, dz'}{\left| \vec{r} - \vec{r}'(t', z') \right|^2 \Big|_{t'=t - \frac{|\vec{r} - \vec{r}'(t', z')|}{c}}} \quad (12)
 \end{aligned}$$

where

$$\cos [\alpha_x(z' = v_e t')] = \frac{x}{\left| \vec{r} - \vec{r}'(t', z' = v_e t') \right| \Big|_{t'=t - \frac{|\vec{r} - \vec{r}'(t', z' = v_e t')|}{c}}}, \quad (13)$$

$$\cos [\alpha_x(z' = v_e t' + L)] = \frac{x}{\left| \vec{r} - \vec{r}'(t', z' = v_e t' + L) \right| \Big|_{t'=t - \frac{|\vec{r} - \vec{r}'(t', z' = v_e t' + L)|}{c}}}, \quad (14)$$

$$\cos [\alpha_y(z' = v_e t')] = \frac{y}{\left| \vec{r} - \vec{r}'(t', z' = v_e t') \right| \Big|_{t'=t - \frac{|\vec{r} - \vec{r}'(t', z' = v_e t')|}{c}}}, \quad (15)$$

$$\cos [\alpha_y(z' = v_e t' + L)] = \frac{y}{\left| \vec{r} - \vec{r}'(t', z' = v_e t' + L) \right| \Big|_{t'=t - \frac{|\vec{r} - \vec{r}'(t', z' = v_e t' + L)|}{c}}}, \quad (16)$$

$$\cos [\alpha_z(z' = v_e t')] = \frac{(z - v_e t')}{\left| \vec{r} - \vec{r}'(t', z' = v_e t') \right| \Big|_{t'=t - \frac{|\vec{r} - \vec{r}'(t', z' = v_e t')|}{c}}}, \quad (17)$$

$$\cos [\alpha_z(z' = v_e t' + L)] = \frac{(z - (v_e t' + L))}{\left| \vec{r} - \vec{r}'(t', z' = v_e t' + L) \right| \Big|_{t'=t - \frac{|\vec{r} - \vec{r}'(t', z' = v_e t' + L)|}{c}}}, \quad (18)$$

and

$$\kappa(z' = v_e t') = \left[ 1 - \frac{v_e}{c} \cos [\alpha_z(z' = v_e t')] \right], \quad (19)$$

$$\kappa(z' = v_e t' + L) = \left[ 1 - \frac{v_e}{c} \cos [\alpha_z(z' = v_e t' + L)] \right] \quad (20)$$

are the retardation factors ([3], p. 246).

The transverse components of the electric field strength  $E_x^p(t', r'(x', y', z'(t'))$ ;  $t, r(x, y, z)$ ) and  $E_y^p(t', r'(x', y', z'(t'))$ ;  $t, r(x, y, z)$ ) are potential relative to the space coordinates, and the longitudinal component  $E_z(t', r'(x', y', z'(t'))$ ;  $t, r(x, y, z)$ ) consists of both a potential component relative to the space coordinates and a dynamic component.

The transverse components of the magnetic field strength  $H_x(t', r'(x', y', z'(t'))$ ;  $t, r(x, y, z)$ ) and  $H_y(t', r'(x', y', z'(t'))$ ;  $t, r(x, y, z)$ ), according to the Eq. (6) and (9), are:

$$\begin{aligned}
 H_x(t', x' = 0, y' = 0, v_e t' < z' < v_e t' + L; t, r(x, y, z)) = \\
 = -\frac{Qv_e^2}{L4\pi c} \frac{\cos [\alpha_y(z' = v_e t')]}{\kappa(z' = v_e t') \left| \vec{r} - \vec{r}'(t', z' = v_e t') \right|} \Big|_{t'=t - \frac{|\vec{r} - \vec{r}'(t', z' = v_e t')|}{c}} \\
 + \frac{Qv_e^2}{L4\pi c} \frac{\cos [\alpha_y(z' = v_e t' + L)]}{\kappa(z' = v_e t' + L) \left| \vec{r} - \vec{r}'(t', z' = v_e t' + L) \right|} \Big|_{t'=t - \frac{|\vec{r} - \vec{r}'(t', z' = v_e t' + L)|}{c}} \\
 - \frac{Qv_e}{L4\pi} \int_{v_e t'}^{v_e t' + L} dz' \frac{\cos [\alpha_y(z')]}{\left| \vec{r} - \vec{r}'(t', z') \right|^2} \Big|_{t'=t - \frac{|\vec{r} - \vec{r}'(t', z')|}{c}}
 \end{aligned} \tag{21}$$

$$\begin{aligned}
 H_y(t', x' = 0, y' = 0, v_e t' < z' < v_e t' + L; t, r(x, y, z)) = \\
 = \frac{Qv_e^2}{L4\pi c} \frac{\cos [\alpha_x(z' = v_e t')]}{\kappa(z' = v_e t') \left| \vec{r} - \vec{r}'(t', z' = v_e t') \right|} \Big|_{t'=t - \frac{|\vec{r} - \vec{r}'(t', z' = v_e t')|}{c}} \\
 - \frac{Qv_e^2}{L4\pi c} \frac{\cos [\alpha_x(z' = v_e t' + L)]}{\kappa(z' = v_e t' + L) \left| \vec{r} - \vec{r}'(t', z' = v_e t' + L) \right|} \Big|_{t'=t - \frac{|\vec{r} - \vec{r}'(t', z' = v_e t' + L)|}{c}} \\
 + \frac{Qv_e}{L4\pi} \int_{v_e t'}^{v_e t' + L} dz' \frac{\cos [\alpha_x(z')]}{\left| \vec{r} - \vec{r}'(t', z') \right|^2} \Big|_{t'=t - \frac{|\vec{r} - \vec{r}'(t', z')|}{c}}
 \end{aligned} \tag{22}$$

The strengths of the electric fields in Eqs. (10)–(12) and magnetic fields with Eqs. (21) and (22), formed by the ends and the main part of the beam, decrease inversely proportional to the first and second powers of the distance from the source point to the observation point.

## 5. Displacement current

We take into account that the displacement current density  $\vec{j}_d(t, r)$  ([7], p. 87):

$$\vec{j}_d(t, r) = \frac{\partial}{\partial t} \vec{D}_d(t, r) = \frac{\partial}{\partial t} \varepsilon_0 \vec{E}(t, r), \tag{23}$$

where the  $\vec{D}_d(t, r) = \varepsilon_0 \vec{E}(t, r)$  is the electric displacement vector. Taking into account the Eqs. (10)–(12) and (23), we get

$$\begin{aligned}
 j_{dx}^p(t', x' = 0, y' = 0, v_e t' < z' < v_e t' + L; t, r(x, y, z)) = \\
 = \frac{Qv_e^2}{L4\pi c} \cos [\alpha_x(z' = v_e t')] \cdot \cos [\alpha_z(z' = v_e t')] \cdot \frac{1}{\kappa^2(z' = v_e t') \left| \vec{r} - \vec{r}'(t', z' = v_e t') \right|^2} \\
 + \frac{Qv_e^3}{L4\pi c^2} \frac{\cos [\alpha_x(z' = v_e t')]}{\kappa^3(z' = v_e t') \left| \vec{r} - \vec{r}'(t', z' = v_e t') \right|^3} \left[ \left| \vec{r} - \vec{r}'(t', z' = v_e t') \right| \right]
 \end{aligned}$$



$$\begin{aligned}
 & - \cos [\alpha_z(z' = v_e t')](z - v_e t') + \\
 & + \frac{Qv_e^2 \cos [\alpha_x(z' = v_e t')] \cos [\alpha_z(z' = v_e t')]}{L4\pi c \kappa^2(z' = v_e t') \left| \vec{r} - \vec{r}'(t', z' = v_e t') \right|^2} - \\
 & - \frac{2Qv_e^2 \cos [\alpha_x(z' = v_e t' + L)] \cdot \cos [\alpha_z(z' = v_e t' + L)]}{L4\pi c \kappa^2(z' = v_e t' + L) \left| \vec{r} - \vec{r}'(t', z' = v_e t' + L) \right|^2} - \\
 & - \frac{Qv_e^3 \cos [\alpha_x(z' = v_e t' + L)]}{L4\pi c^2 \kappa^3(z' = v_e t' + L) \left| \vec{r} - \vec{r}'(t', z' = v_e t' + L) \right|^3} \\
 & \cdot \left[ \left| \vec{r} - \vec{r}'(t', z' = v_e t' + L) \right| - \cos [\alpha_z(z' = v_e t' + L)] \cdot (z - (v_e t' + L)) \right] + \\
 & + \frac{Qv_e \cos [\alpha_x(z' = v_e t' + L)]}{L4\pi \kappa^2(z' = v_e t' + L) \left| \vec{r} - \vec{r}'(t', z' = v_e t' + L) \right|^2} - \\
 & - \frac{Qv_e \cos [\alpha_x(z' = v_e t')]}{L4\pi \kappa^2(z' = v_e t') \left| \vec{r} - \vec{r}'(t', z' = v_e t') \right|^2} \tag{24}
 \end{aligned}$$

$$\begin{aligned}
 & j_{dy}^p(t', x' = 0, y' = 0, v_e t' < z' < v_e t' + L; t, r(x, y, z)) = \\
 & = \frac{Qv_e^2 \cos [\alpha_y(z' = v_e t')] \cdot \cos [\alpha_z(z' = v_e t')]}{L4\pi c} \cdot \\
 & \cdot \frac{1}{\kappa^2(z' = v_e t') \left| \vec{r} - \vec{r}'(t', z' = v_e t') \right|^2} + \frac{Qv_e^3 \cos [\alpha_y(z' = v_e t')]}{L4\pi c^2 \kappa^3(z' = v_e t') \left| \vec{r} - \vec{r}'(t', z' = v_e t') \right|^3} \\
 & \left[ \left| \vec{r} - \vec{r}'(t', z' = v_e t') \right| - \cos [\alpha_z(z' = v_e t')](z - v_e t') \right] + \\
 & + \frac{Qv_e^2 \cos [\alpha_y(z' = v_e t')] \cos [\alpha_z(z' = v_e t')]}{L4\pi c \kappa^2(z' = v_e t') \left| \vec{r} - \vec{r}'(t', z' = v_e t') \right|^2} - \\
 & - \frac{2Qv_e^2 \cos [\alpha_y(z' = v_e t' + L)] \cdot \cos [\alpha_z(z' = v_e t' + L)]}{L4\pi c \kappa^2(z' = v_e t' + L) \left| \vec{r} - \vec{r}'(t', z' = v_e t' + L) \right|^2} - \frac{Qv_e^3}{L4\pi c^2} \\
 & \frac{\cos [\alpha_y(z' = v_e t' + L)]}{\kappa^3(z' = v_e t' + L) \left| \vec{r} - \vec{r}'(t', z' = v_e t' + L) \right|^3} \left[ \left| \vec{r} - \vec{r}'(t', z' = v_e t' + L) \right| \right. \\
 & \left. - \cos [\alpha_z(z' = v_e t' + L)] \cdot (z - (v_e t' + L)) \right] \\
 & + \frac{Qv_e \cos [\alpha_y(z' = v_e t' + L)]}{L4\pi \kappa^2(z' = v_e t' + L) \left| \vec{r} - \vec{r}'(t', z' = v_e t' + L) \right|^2} - \\
 & - \frac{Qv_e \cos [\alpha_y(z' = v_e t')]}{L4\pi \kappa^2(z' = v_e t') \left| \vec{r} - \vec{r}'(t', z' = v_e t') \right|^2} \tag{25}
 \end{aligned}$$

$$\begin{aligned}
 & j_{dz}(t', x' = 0, y' = 0, v_e t' < z' < v_e t' + L; t, r(x, y, z)) = \\
 & = \frac{-Qv_e^2 \sin^2 [\alpha_z(z' = v_e t')]}{L4\pi c} \cdot
 \end{aligned}$$



$$\begin{aligned}
 & \frac{1}{\kappa^2(z' = v_e t') \left| \vec{r} - \vec{r}'(t', z' = v_e t') \right|^2} + \frac{Qv_e^3 \cos [\alpha_z(z' = v_e t')]}{L4\pi c^2 \kappa^3(z' = v_e t') \left| \vec{r} - \vec{r}'(t', z' = v_e t') \right|^3} \cdot \\
 & \cdot \left[ \left| \vec{r} - \vec{r}'(t', z' = v_e t') \right| - \cos [\alpha_z(z' = v_e t')](z - v_e t') \right] \\
 & + \frac{Qv_e^2 \cos^2 [\alpha_z(z' = v_e t')]}{L4\pi c \kappa^2(z' = v_e t') \left| \vec{r} - \vec{r}'(t', z' = v_e t') \right|^2} \\
 & \frac{Qv_e^2 \sin^2 [\alpha_z(z' = v_e t' + L)]}{L4\pi c \kappa^2(z' = v_e t' + L) \left| \vec{r} - \vec{r}'(t', z' = v_e t' + L) \right|^2} + \frac{Qv_e^3}{L4\pi c^2} \cdot \\
 & \cdot \frac{\cos [\alpha_z(z' = v_e t' + L)]}{\kappa^2(z' = v_e t' + L) \left| \vec{r} - \vec{r}'(t', z' = v_e t' + L) \right|^3} \\
 & \cdot \left[ \left| \vec{r} - \vec{r}'(t', z' = v_e t' + L) \right| - \cos [\alpha_z(z' = v_e t' + L)] \cdot \right. \\
 & \left. \cdot (z - (v_e t' + L)) \right] + \frac{Qv_e^2 \cos^2 [\alpha_z(z' = v_e t' + L)]}{L4\pi c \kappa^2(z' = v_e t' + L) \left| \vec{r} - \vec{r}'(t', z' = v_e t' + L) \right|^2} - \\
 & \frac{Qv_e^4}{L4\pi c^3 \kappa^3(z' = v_e t') \left| \vec{r} - \vec{r}'(t', z' = v_e t') \right|^3} \left[ \left| \vec{r} - \vec{r}'(t', z' = v_e t') \right| - \cos [\alpha_z(z' = v_e t')](z - v_e t') \right] - \\
 & - \frac{Qv_e^3 \cos [\alpha_z(z' = v_e t')]}{L4\pi c^2 \kappa^2(z' = v_e t') \left| \vec{r} - \vec{r}'(t', z' = v_e t') \right|^2} \\
 & + \frac{Qv_e^4}{L4\pi c^3 \kappa^3(z' = v_e t' + L) \left| \vec{r} - \vec{r}'(t', z' = v_e t' + L) \right|^3} \cdot \\
 & \cdot \left[ \left| \vec{r} - \vec{r}'(t', z' = v_e t' + L) \right| - \cos [\alpha_z(z' = v_e t' + L)](z - (v_e t' + L)) \right] + \\
 & + \frac{Qv_e^3 \cos [\alpha_z(z' = v_e t' + L)]}{L4\pi c^2 \kappa^2(z' = v_e t' + L) \left| \vec{r} - \vec{r}'(t', z' = v_e t' + L) \right|^2} \\
 & - \frac{Qv_e \cos [\alpha_z(z' = v_e t')]}{L4\pi \kappa(z' = v_e t') \left| \vec{r} - \vec{r}'(t', z' = v_e t') \right|^2} \tag{26}
 \end{aligned}$$

The transverse components of the displacement current density  $j_{dx}^p(t', r'(x', y', z'(t')); t, r(x, y, z))$  and  $j_{dy}^p(t', r'(x', y', z'(t')); t, r(x, y, z))$  are potential with respect to space coordinates, and the longitudinal component  $j_{dz}^p(t', r'(x', y', z'(t')); t, r(x, y, z))$  consists of potential and dynamic components. Displacement current densities are decreasing inversely proportional to the second power of the distance from the source point to the observation point.

## 6. Flux of electrical energy

The electrical energy flux density per unit time  $\vec{S}^\psi(t, r)$ , according to ([10], p. 125) Eq. (15) and [11] Eqs. (7) and (8), has the form

$$\vec{S}^\psi(t, r) = \psi(t, r) \cdot \vec{j}_d(t, r) \quad (27)$$

Taking into account the Eq. (5) or the Eq. (7) and the Eqs. (24)–(26), we can write

$$\begin{aligned} S_x^\psi(t', x' = 0, y' = 0, v_e t' < z' < v_e t' + L; t, r(x, y, z)) &= \\ &= \psi(t', x' = 0, y' = 0, v_e t' < z' < v_e t' + L; t, r(x, y, z)) \cdot \\ & j_{dx}^p(t', x' = 0, y' = 0, v_e t' < z' < v_e t' + L; t, r(x, y, z)) \end{aligned} \quad (28)$$

$$\begin{aligned} S_y^\psi(t', x' = 0, y' = 0, v_e t' < z' < v_e t' + L; t, r(x, y, z)) &= \\ &= \psi(t', x' = 0, y' = 0, v_e t' < z' < v_e t' + L; t, r(x, y, z)) \cdot \\ & \cdot j_{dy}^p(t', x' = 0, y' = 0, v_e t' < z' < v_e t' + L; t, r(x, y, z)) \end{aligned} \quad (29)$$

$$\begin{aligned} S_z^\psi(t', x' = 0, y' = 0, v_e t' < z' < v_e t' + L; t, r(x, y, z)) &= \\ &= \psi(t', x' = 0, y' = 0, v_e t' < z' < v_e t' + L; t, r(x, y, z)) \cdot \\ & j_{dz}^p(t', x' = 0, y' = 0, v_e t' < z' < v_e t' + L; t, r(x, y, z)) \end{aligned} \quad (30)$$

The electrical energy flux density  $\vec{S}^\psi(t, r)$  decreases inversely proportional to the third power of the distance from the source point to the observation point. The electrical energy flux per unit time into a given solid angle decreases inversely proportional to the first power of the distance from the source point to the observation point. The flux takes place both in the near and the intermediate zones.

## 7. Pointing vector

The Poynting vector or the flux density of electromagnetic energy per unit time is determined by the formula ([3], p. 259)

$$\vec{S}(t, r) = \vec{E}(t, r) \times \vec{H}(t, r) \quad (31)$$

The Poynting vector along the  $Ox$  axis estimated according to Eq. (31) with the help of Eqs. (12) and (22) may be written as follows:

$$\begin{aligned} S_x(t', x' = 0, y' = 0, v_e t' < z' < v_e t' + L; t, r(x, y, z)) &= \\ &= -E_z(t', x' = 0, y' = 0, v_e t' < z' < v_e t' + L; t, r(x, y, z)) \cdot \\ & \cdot H_y(t', x' = 0, y' = 0, v_e t' < z' < v_e t' + L; t, r(x, y, z)) \\ &= -\{E_z^p(z' = v_e t') + E_z^p(z' = v_e t' + L) \\ & + E_z^r(z' = v_e t') + E_z^r(v_e t' < z' < v_e t' + L)\} \cdot \\ & \left\{ H_y(z' = v_e t') + H_y(z' = v_e t' + L) + H_y^c(v_e t' < z' < v_e t' + L) \right\} \end{aligned} \quad (32)$$

where the summands in curly brackets are defined by Eq. (12) and Eq. (22), respectively. Rewriting the Eq. (32) in the following form:

$$\begin{aligned} S_x(t', x' = 0, y' = 0, v_e t' < z' < v_e t' + L; t, r(x, y, z)) \\ = {}^i S_x(z' = v_e t', z' = v_e t' + L) + {}^{pi} S_x(z' = v_e t', z' = v_e t' + L, v_e t' < z' < v_e t' + L) \\ + {}^f S_x^c(v_e t' < z' < v_e t' + L), \end{aligned} \quad (33)$$

where the  ${}^i S_x(z' = v_e t', z' = v_e t' + L)$  there is a flux of electromagnetic energy in a unit time that goes into the wave zone, the  ${}^{pi} S_x(z' = v_e t', z' = v_e t' + L, v_e t' < z' < v_e t' + L)$  there is a flux of electromagnetic energy in the intermediate zone, the  ${}^f S_x^c(v_e t' < z' < v_e t' + L)$  there is a flux of electromagnetic energy in the near zone. As this takes place

$$\begin{aligned} {}^i S_x(z' = v_e t', z' = v_e t' + L) = {}^i S_x(z' = v_e t') + \\ + {}^i S_x(z' = v_e t' + L) + {}^i S_x^{WA}(z' = v_e t', z' = v_e t' + L), \end{aligned} \quad (34)$$

$$\begin{aligned} {}^i S_x(z' = v_e t') = {}^i S_x^{WA}(z' = v_e t') + {}^i S_x^A(z' = v_e t') = \\ = -E_z^p(z' = v_e t') \cdot H_y(z' = v_e t') - E_z^r(z' = v_e t') \cdot H_y(z' = v_e t'), \end{aligned} \quad (35)$$

$$\begin{aligned} {}^i S_x(z' = v_e t' + L) = {}^i S_x^{WA}(z' = v_e t' + L) + {}^i S_x^A(z' = v_e t' + L) = \\ -E_z^p(z' = v_e t' + L) \cdot H_y(z' = v_e t' + L) - E_z^r(z' = v_e t' + L) \cdot H_y(z' = v_e t' + L), \end{aligned} \quad (36)$$

$$\begin{aligned} {}^i S_x^{WA}(z' = v_e t', z' = v_e t' + L) = -E_z^p(z' = v_e t') \cdot H_y(z' = v_e t' + L) - E_z^p(z' = v_e t' + L) \\ \cdot H_y(z' = v_e t') - E_z^r(z' = v_e t') \cdot H_y(z' = v_e t' + L) \\ - E_z^r(z' = v_e t' + L) \cdot H_y(z' = v_e t'). \end{aligned} \quad (37)$$

The energy fluxes,  ${}^i S_x(z' = v_e t')$ ,  ${}^i S_x(z' = v_e t' + L)$ ,  ${}^i S_x^{WA}(z' = v_e t', z' = v_e t' + L)$ , are determined by point sources of radiation at the REB segment beginning, the REB segment end, and the REB segment interference, respectively.

$$\begin{aligned} {}^{pi} S_x(z' = v_e t', z' = v_e t' + L, v_e t' < z' < v_e t' + L) = \\ -E_z^p(z' = v_e t') \cdot H_y^c(v_e t' < z' < v_e t' + L) - E_z^p(z' = v_e t' + L) \cdot H_y^c(v_e t' < z' < v_e t' + L) \\ - E_z^r(z' = v_e t') \cdot H_y^c(v_e t' < z' < v_e t' + L) - E_z^r(z' = v_e t' + L) \cdot H_y^c(v_e t' < z' < v_e t' + L) \\ E_z^c(v_e t' < z' < v_e t' + L) \cdot H_y(z' = v_e t') - E_z^c(v_e t' < z' < v_e t' + L) \cdot H_y(z' = v_e t' + L). \end{aligned} \quad (38)$$

$${}^f S_x^c(v_e t' < z' < v_e t' + L) = -E_z^c(v_e t' < z' < v_e t' + L) \cdot H_y^c(v_e t' < z' < v_e t' + L). \quad (39)$$

The Poynting vector along the Oy axis, taking into account Eqs. (12), (21), (31), similarly to Eqs. (33)–(39), is represented by:

$$\begin{aligned} S_y(t', x' = 0, y' = 0, v_e t' < z' < v_e t' + L; t, r(x, y, z)) = {}^i S_y(z' = v_e t', z' = v_e t' + L) + \\ + {}^{pi} S_y(z' = v_e t', z' = v_e t' + L, v_e t' < z' < v_e t' + L) + {}^f S_y^c(v_e t' < z' < v_e t' + L), \end{aligned} \quad (40)$$

$$\begin{aligned} {}^i S_y(z' = v_e t', z' = v_e t' + L) = {}^i S_y(z' = v_e t') + {}^i S_y(z' = v_e t' + L) + \\ + {}^i S_y^{WA}(z' = v_e t', z' = v_e t' + L) \end{aligned} \quad (41)$$

$$\begin{aligned} {}^iS_y(z' = v_et') &= {}^iS_y^{\psi A}(z' = v_et') + {}^iS_y^A(z' = v_et') = \\ &= E_z^p(z' = v_et') \cdot H_x(z' = v_et') + E_z^r(z' = v_et') \cdot H_x(z' = v_et') \end{aligned} \quad (42)$$

$$\begin{aligned} {}^iS_y(z' = v_et' + L) &= {}^iS_y^{\psi A}(z' = v_et' + L) + {}^iS_y^A(z' = v_et' + L) = \\ &= E_z^p(z' = v_et' + L) \cdot H_x(z' = v_et' + L) + E_z^r(z' = v_et' + L) \cdot H_x(z' = v_et' + L), \end{aligned} \quad (43)$$

$$\begin{aligned} {}^iS_y^{\psi A}(z' = v_et', z' = v_et' + L) &= E_z^p(z' = v_et') \cdot H_x(z' = v_et' + L) + E_z^p(z' = v_et' + L) \cdot \\ &\cdot H_x(z' = v_et') + E_z^r(z' = v_et') \cdot H_x(z' = v_et' + L) + E_z^r(z' = v_et' + L) \cdot H_x(z' = v_et'), \end{aligned} \quad (44)$$

$$\begin{aligned} {}^{pi}S_y(z' = v_et', z' = v_et' + L, v_et' < z' < v_et' + L) &= \\ E_z^p(z' = v_et') \cdot H_x^c(v_et' < z' < v_et' + L) &+ E_z^p(z' = v_et' + L) \cdot H_x^c(v_et' < z' < v_et' + L) + \\ + E_z^r(z' = v_et') \cdot H_x^c(v_et' < z' < v_et' + L) &+ E_z^r(z' = v_et' + L) \cdot H_x^c(v_et' < z' < v_et' + L) + \\ + E_x^c(v_et' < z' < v_et' + L) \cdot H_x(z' = v_et') &+ E_x^c(v_et' < z' < v_et' + L) \cdot H_x(z' = v_et' + L), \end{aligned} \quad (45)$$

$${}^fS_y^c(v_et' < z' < v_et' + L) = -E_x^c(v_et' < z' < v_et' + L) \cdot H_x^c(v_et' < z' < v_et' + L). \quad (46)$$

The Poynting vector along the Oz axis, taking into account Eqs. (10), (11), (21), (22), and (31), may be written as follows:

$$\begin{aligned} S_z(t', x' = 0, y' = 0, v_et' < z' < v_et' + L; t, r(x, y, z)) &= {}^iS_z(z' = v_et', z' = v_et' + L) + \\ + {}^{pi}S_z(z' = v_et', z' = v_et' + L, v_et' < z' < v_et' + L) &+ {}^fS_z^c(v_et' < z' < v_et' + L), \end{aligned} \quad (47)$$

$$\begin{aligned} {}^iS_z(z' = v_et', z' = v_et' + L) &= {}^iS_z(z' = v_et') + \\ + {}^iS_z(z' = v_et' + L) &+ {}^iS_z^{\psi A}(z' = v_et', z' = v_et' + L) \end{aligned} \quad (48)$$

$$\begin{aligned} {}^iS_z(z' = v_et') &= {}^iS_z^{\psi A}(z' = v_et') = \\ = E_x^p(z' = v_et') \cdot H_y(z' = v_et') - E_y^p(z' = v_et') \cdot H_x(z' = v_et') \end{aligned} \quad (49)$$

$$\begin{aligned} {}^iS_z(z' = v_et' + L) &= {}^iS_z^{\psi A}(z' = v_et' + L) = \\ = E_x^p(z' = v_et' + L) \cdot H_y(z' = v_et' + L) - E_y^p(z' = v_et' + L) \cdot H_x(z' = v_et' + L) \end{aligned} \quad (50)$$

$$\begin{aligned} {}^iS_z^{\psi A}(z' = v_et', z' = v_et' + L) &= E_x^p(z' = v_et') \cdot H_y(z' = v_et' + L) + \\ + E_x^p(z' = v_et' + L) \cdot H_y(z' = v_et') - E_y^p(z' = v_et') \cdot H_x(z' = v_et' + L) - \\ - E_y^p(z' = v_et' + L) \cdot H_x(z' = v_et') \end{aligned} \quad (51)$$

$$\begin{aligned} {}^{pi}S_z(z' = v_et', z' = v_et' + L, v_et' < z' < v_et' + L) &= \\ E_x^p(z' = v_et') \cdot H_y^c(v_et' < z' < v_et' + L) &+ E_x^p(z' = v_et' + L) \cdot H_y^c(v_et' < z' < v_et' + L) + \\ + E_x^c(v_et' < z' < v_et' + L) \cdot H_y(z' = v_et') &+ E_x^c(v_et' < z' < v_et' + L) \cdot H_y(z' = v_et' + L) - \\ - E_y^p(z' = v_et') \cdot H_x^c(v_et' < z' < v_et' + L) - E_y^p(z' = v_et' + L) \cdot H_x^c(v_et' < z' < v_et' + L) - \\ - E_y^c(v_et' < z' < v_et' + L) \cdot H_x(z' = v_et') - E_y^c(v_et' < z' < v_et' + L) \cdot H_x(z' = v_et' + L), \end{aligned} \quad (52)$$

$$\begin{aligned} {}^fS_z^c(v_et' < z' < v_et' + L) &= E_x^c(v_et' < z' < v_et' + L) \cdot H_y^c(v_et' < z' < v_et' + L) - \\ - E_x^c(v_et' < z' < v_et' + L) \cdot H_x^c(v_et' < z' < v_et' + L). \end{aligned} \quad (53)$$

## 8. Numerical results

We have considered the filamentary REB of the length  $L = 3 \text{ m}$ , moving along the  $Oz$  axis with velocity  $v_e = 0.94 c$  ( $c$  is the speed of light) and having overall charge  $Q = (-1) \cdot 10^{-10} \text{ C}$ .

In the laboratory coordinate system, the dependence of the electric field strength  $E_x^p(t' = 0, x' = 0, y' = 0, z' = 0; t, r(x, y = 0, z = 0))$ , radiated by the beginning of the REB segment  $r'(x' = 0, y' = 0, z' = 0)$ , on the transverse coordinate  $x$  was calculated using Eq. (10), (**Figure 1**). The signal radiation time  $t'$  was selected equal to zero  $t' = 0$ . The observation point  $r(x, y = 0, z = 0)$  was selected in the cross section  $z = 0$  at  $y = 0$ . The observation time  $t$  was determined by the formula  $t = \frac{|x|}{c}$ .

The dependence of the potential electric field strength  $E_x^p(t', x' = 0, y' = 0, z' = v_e t'; t, r(x = 0.3 \text{ m}, y = 0, z = 0))$ , radiated by the beginning of the REB segment  $r'(x' = 0, y' = 0, z' = v_e t')$ , on the signal generation time  $t'$  calculated with the help of Eq. (10), is represented in **Figure 2** where  $r(x = 0.3 \text{ m}, y = 0, z = 0)$  is the observation point coordinates.

The dependence of the magnetic field strength  $H_y(t' = 0, x' = 0, y' = 0, z' = L; t, r(x, y = 0, z = 0))$  radiated by the REB segment end  $r'(x' = 0, y' = 0, z' = L)$  on the transverse coordinate  $x$  was calculated using Eq. (22) (**Figure 3**). The signal

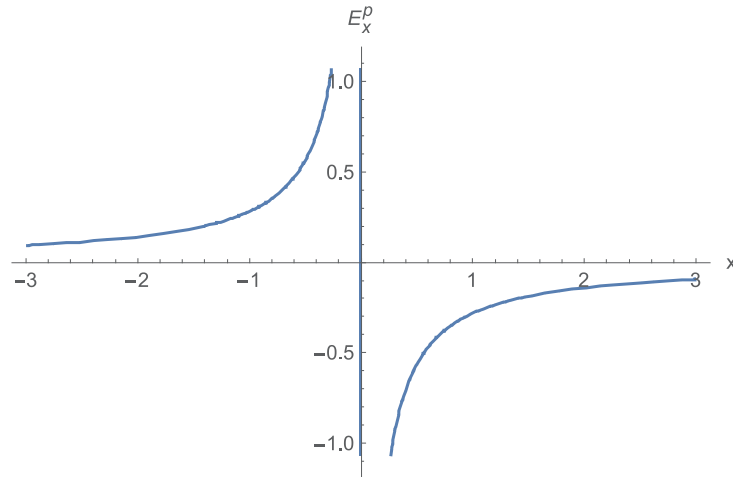


**Figure 1.**

The potential electric field strength  $E_x^p(t' = 0, x' = 0, y' = 0, z' = 0; t, r(x, y = 0, z = 0))$  radiated by the REB segment beginning.

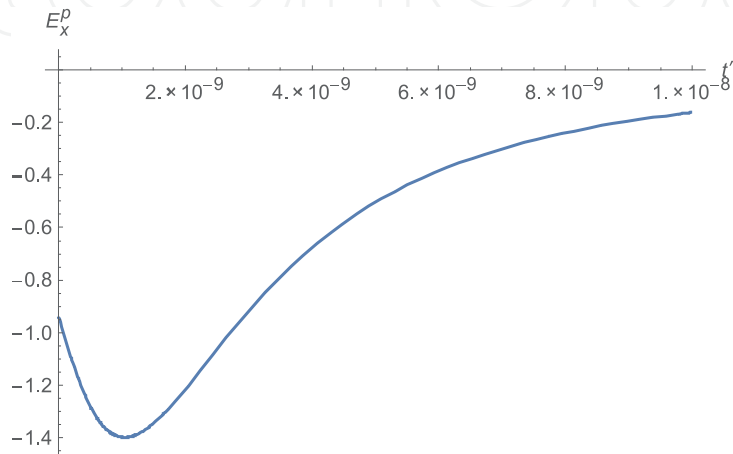


**Figure 2.**

The potential electric field strength  $E_x^p(t', x' = 0, y' = 0, z' = v_e t'; t, r(x = 0.3 \text{ m}, y = 0, z = 0))$  radiated by the REB segment beginning.

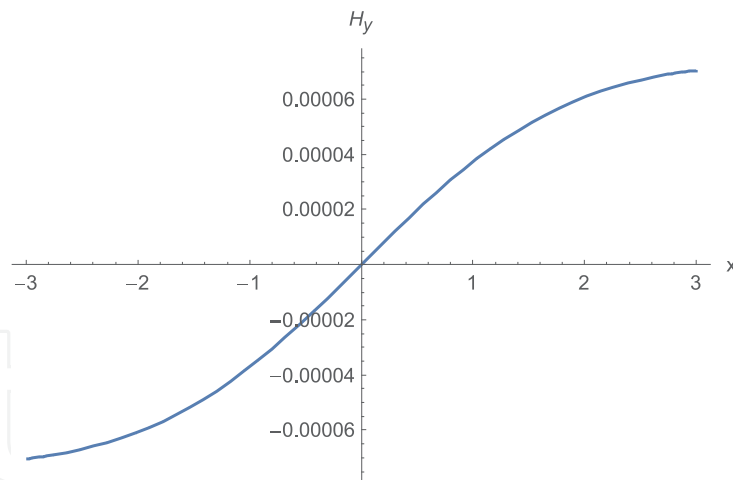


**Figure 3.** Magnetic field strength  $H_y(t' = 0, x' = 0, y' = 0, z' = L; t, r(x, y = 0, z = 0))$  radiated by the REB segment end.

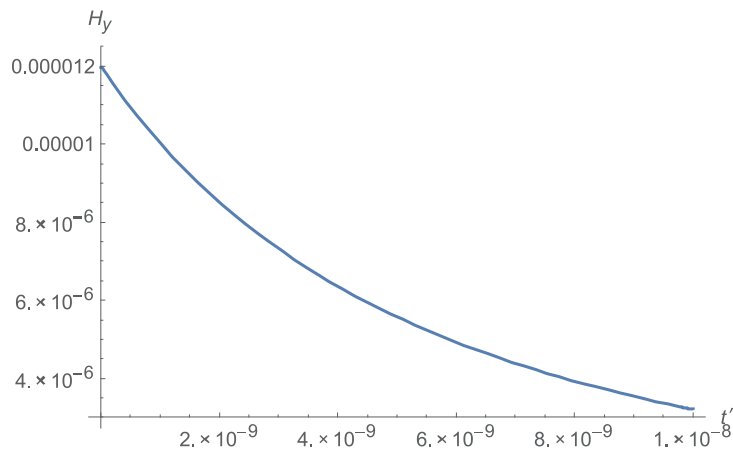


**Figure 4.** Magnetic field strength  $H_y(t', x' = 0, y' = 0, z' = v_e t' + L; t, r(x = 0.3m, y = 0, z = 0))$  radiated by the REB segment end.

generation time  $t'$  was selected equal to the zero,  $t' = 0$  where  $r(x = 0.3m, y = 0, z = 0)$  is the observation point coordinates. The observation time  $t$  was determined by the formula  $t = \frac{\sqrt{x^2 + L^2}}{c}$ .

The dependence of the magnetic field strength  $H_y(t', x' = 0, y' = 0, z' = v_e t' + L; t, r(x = 0.3m, y = 0, z = 0))$ , radiated by the REB segment end  $r'(x' = 0, y' = 0, z' = v_e t' + L)$ , on the signal radiation time  $t'$  calculated using Eq.(22), is represented in **Figure 4** where  $r(x = 0.3m, y = 0, z = 0)$  is the observation point coordinates.

The dependence of the electromagnetic energy flux  $^i S_z(t' = 0, x' = 0, y' = 0, z' = 0; t, r(x, y = 0, z = 0))$ , radiated by the REB segment beginning  $r'(x' = 0, y' = 0, z' = 0)$ , on the transverse coordinate  $x$  was calculated with the help of Eqs. (49), (10), (11), (21), and (22) (**Figure 5**). The signal generation time  $t'$  was selected equal to the zero,  $t' = 0$ . The  $r(x, y = 0, z = 0)$  is the observation point coordinates. The observation time  $t$  was determined by the formula  $t = \frac{|x|}{c}$ .

The dependence of the electromagnetic energy flux  $^i S_z(t', x' = 0, y' = 0, z' = v_e t'; t, r(x = 0.3m, y = 0, z = 0))$ , radiated by the REB segment  $r'(x' = 0, y' = 0, z' = v_e t')$ , on the signal generation time  $t'$ , calculated by Eqs. (49),

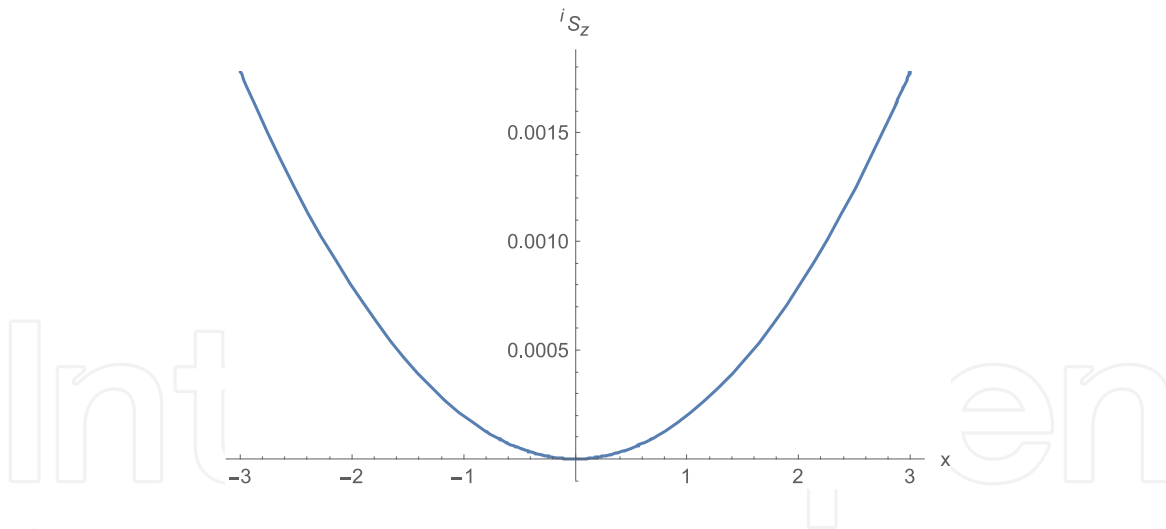


**Figure 5.**

The electromagnetic energy flux  $iS_z(t' = 0, x' = 0, y' = 0, z' = 0; t, r(x, y = 0, z = 0))$  radiated by the REB segment beginning.

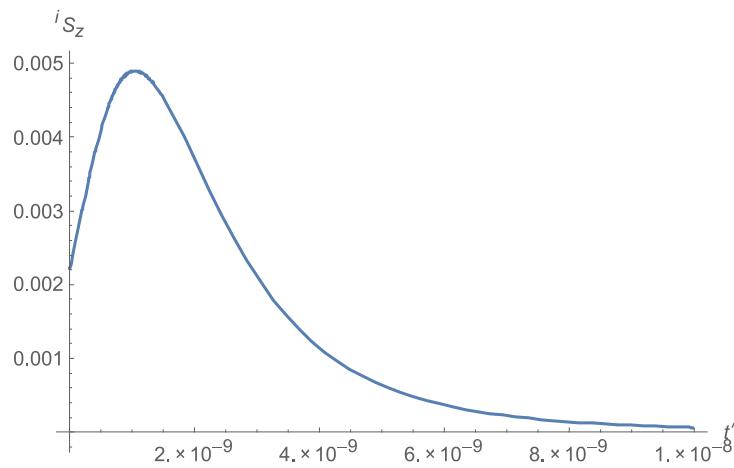


**Figure 6.**

The electromagnetic energy flux  $iS_z(t', x' = 0, y' = 0, z' = v_e t'; t, r(x = 0.3m, y = 0, z = 0))$  radiated by the REB segment beginning.

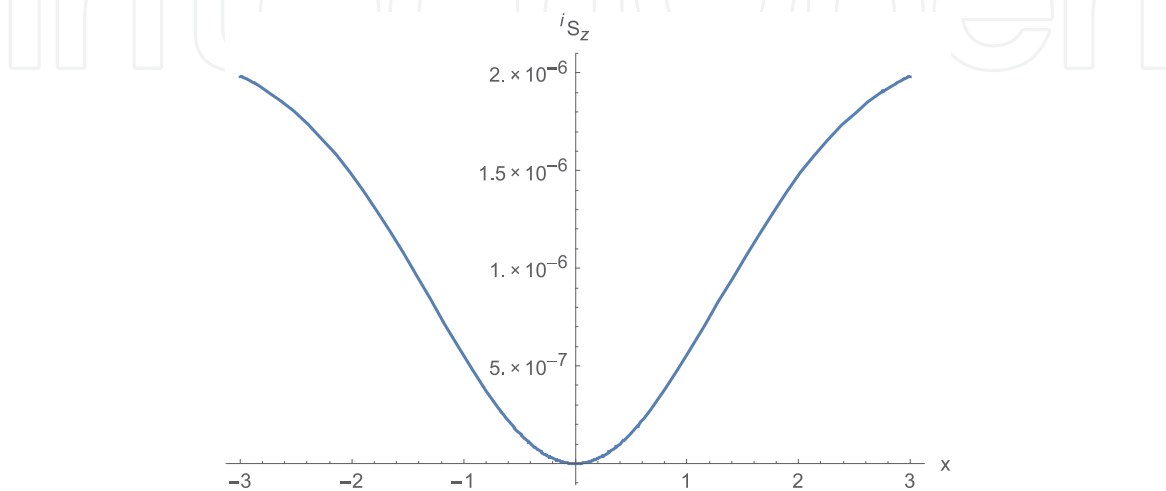


**Figure 7.**

The electromagnetic energy flux  $iS_z(t' = 0, x' = 0, y' = 0, z' = L; t, r(x, y = 0, z = 0))$  radiated by the REB segment end.



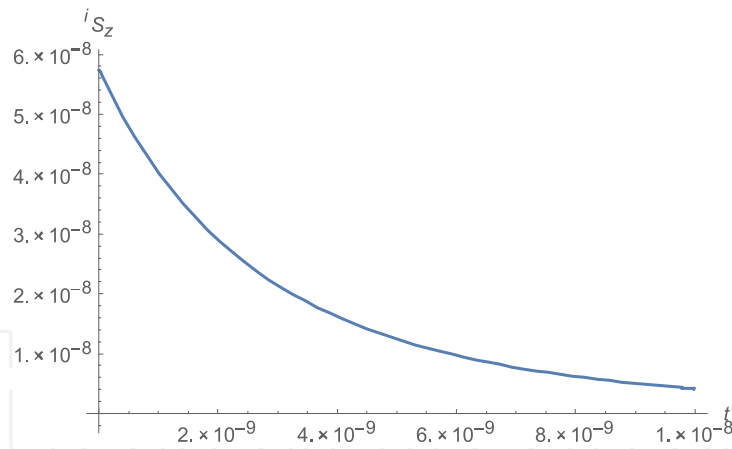


**Figure 8.**

The electromagnetic energy flux  $iS_z(t', x' = 0, y' = 0, z' = v_e t' + L; t, r(x = 0.3m, y = 0, z = 0))$  radiated by the REB segment end.

(10), (11), (21), (22), is shown in **Figure 6**. The observation point coordinate is  $r(x = 0.3m, y = 0, z = 0)$ .

The dependence of the electromagnetic energy flux  $iS_z(t' = 0, x' = 0, y' = 0, z' = L; t, r(x, y = 0, z = 0))$ , radiated by the REB segment end  $r'(x' = 0, y' = 0, z' = L)$ , on the transverse coordinate  $x$  was calculated with the help of Eqs. (50), (10), (11), (21), (22) (**Figure 7**). The signal radiation time  $t'$  was selected equal to the zero  $t' = 0$ . The  $r(x, y = 0, z = 0)$  is the observation point coordinates. The observation time  $t$  was determined by the formula  $t = \frac{\sqrt{x^2 + L^2}}{c}$ .

The dependence of the electromagnetic energy flux  $iS_z(t', x' = 0, y' = 0, z' = v_e t' + L; t, r(x = 0.3m, y = 0, z = 0))$ , radiated by the REB segment end  $r'(x' = 0, y' = 0, z' = v_e t' + L)$ , on the signal radiation time  $t'$ , calculated according to Eqs. (50), (10), (11), (21), (22), is shown in **Figure 8** where  $r(x = 0.3m, y = 0, z = 0)$  is the observation point coordinates.

## 9. Conclusions

The applicability of relativity in the physics of charged particle beams has been shown from the example of radiation by a filamentary REB segment uniformly moving in vacuum along a linear direction.

In electrodynamics, in a moving coordinate system, the relative distance between a charged object and an observer does not change. The phenomenon of relativity associated with the field dynamics degenerates to electrostatic processes. In rest, or laboratory, coordinate system, the relative distance is changing with time, the charge density also varies with the time, and as a result, the retardation phenomena came to the scene and the Poisson equation is to be substituted by the wave equation.

The expressions have been obtained to describe the strengths of the electric and magnetic fields and the electric and electromagnetic energy fluxes in all three zones: near field zone, intermediate, and wave zones. The filamentary REB edges are relativistic point-like sources of electromagnetic energy propagating in the wave zone. The REB edges form a potential component of the electric field strength, which is inversely proportional to the distance from the source point to the observation point. In the wave zone, strength of this field is comparable with that of the dynamic component of the electric field.

The dynamic component of the electric field strength and the axially symmetric magnetic field form both a constant flux into the given solid angle, i.e. electromagnetic radiation, and a flux per time unit directed along the normal to the conical surface of the above solid angle. The potential component of the electric field, directed along the radius, and the axially symmetric magnetic field form a flux oriented along the polar direction, i.e., along the normal to the conical surface. The fluxes crossing the above conical surface are independent of the distance between the source point and the observation point. In the wave zone, the radiations from the beginning and end of the REB segment are added up, while the fluxes through the above conical surface caused by dynamic and potential components of electric field, are subtracted.

Relativistic point-like sources create in the wave zone the vortex components of the magnetic field. The REB edges radiate hybrid electromagnetic waves, comprising of potential and vortex electric fields, as well as a vortex magnetic field. The electric and magnetic field strengths radiated by the REB segment edges have opposite signs. In the wave zone, the radiated electromagnetic field fluxes are compound of the electromagnetic energy fluxes, produced by both the REB segment beginning and its end, as well as of their interference components. In the intermediate zone, the electrical energy flux takes place due to the electric potential field and the displacement current. The REB segment, between the beam edges, having a constant charge density, produces a quasi-static electromagnetic field in the near zone.

## Acknowledgements

This work was funded in part by NATO research project G5465 within frames of the Science for Peace and Security (SPS) program.

## Author details

Sergey Prijmenko<sup>1\*</sup> and Konstantin Lukin<sup>2,3\*</sup>


<sup>1</sup> Institute for Plasma Electronics and New Methods of Acceleration, National Science Center Kharkov Institute of Physics and Technology, National Academy of Science of Ukraine, Kharkov, Ukraine

<sup>2</sup> Usikov Institute for Radiophysics and Electronics, National Academy of Science of Ukraine, Kharkov, Ukraine

<sup>3</sup> Faculty of Electrical Engineering and Informatics, University of Pardubice, Pardubice, Czech Republic

\*Address all correspondence to: [sprijmenko@kipt.kharkov.ua](mailto:sprijmenko@kipt.kharkov.ua) and [lukin.konstantin@gmail.com](mailto:lukin.konstantin@gmail.com)

## IntechOpen

© 2019 The Author(s). Licensee IntechOpen. This chapter is distributed under the terms of the Creative Commons Attribution License (<http://creativecommons.org/licenses/by/3.0>), which permits unrestricted use, distribution, and reproduction in any medium, provided the original work is properly cited. 

## References

- [1] Landau LD, Lifshitz EM. The Classical Theory of Fields (Volume 2: A Course of Theoretical Physics). Pergamon Press; 1971
- [2] de Sangro R, Finocchiaro G, Patteri P, Piccolo M, Pizzella G. Measuring propagation speed of Coulomb fields. The European Physical Journal C. 2015;75:137. DOI: 10.1140/epic/s10052-015-3355-3
- [3] Jackson JD. Classical Electrodynamics. New York: John Wiley; 1998. 537p
- [4] Meshkov IN, Chirikov BV. Relativistic Electrodynamics. Novosibirsk: Vysshaya Shkola, NSU; 1982. 80p (in Russian)
- [5] Purcell E. Electricity and Magnetism (Berkeley Physics Course, Vol. 2). 2nd ed. McGraw-Hill Science/Engineering/Math; 1984. 506p
- [6] Jefimenko OD. Retardation and relativity: The case of a moving line charge. American Journal of Physics. 1995;63(5):454-459
- [7] Akhiezer AI, Akhiezer IA. Electromagnetism and Electromagnetic Waves. Moscow: Vysshaya Shkola; 1985. 594p (in Russian)
- [8] Dwight HB. Tables of Integrals and Other Mathematical Data. New York: The Macmillan Company; 1957. p. 172
- [9] Madelung E. Mathematical Apparatus of Physics. Moscow: Nauka; 1968. 618p (in Russian)
- [10] Stratton JA. Electromagnetic Theory. Moscow-Leningrad: Ogiz-Gostekhizdat; 1948. 539p (in Russian)
- [11] Prijmenko SD, Lukin KA. The flow of electromagnetic energy in the presence of potential electric and magnetic fields. Applied Radio Electronics. 2018;17(1, 2):28-34 (in Russian)